Soliton interaction in a complex plasma

P. Harvey,[1] C. Durniak,[1] D. Samsonov,[1] and G. Morfill[2]

[1]*Department of Electrical Engineering and Electronics, The University of Liverpool, Liverpool L69 3GJ, United Kingdom*
[2]*Max-Planck-Institut für Extraterrestrische Physik, D-85740 Garching, Germany*

The interaction of two counterpropagating solitons of equal amplitudes has been studied experimentally and numerically in a monolayer strongly coupled complex plasma. Complex plasmas are microparticle suspensions in ion-electron plasmas. It was found that the solitons are delayed after the collision. Solitons with higher amplitude experience longer delays. The amplitude of the overlapping solitons during the collision was less than the sum of the initial soliton amplitudes.

PACS number(s): 52.27.Lw, 52.35.Fp

In a complex (dusty) plasma, particles ranging from nanometer to micrometer sizes are introduced into an electron-ion plasma. The particles become charged and interact collectively, arranging themselves to form orderly structures [1–4]. Complex plasmas exist in gas, liquid, and crystalline states. They also sustain different kinds of linear and nonlinear waves.

A soliton or a solitary wave is a localized wave that retains its shape as it propagates through a medium. It was observed first by Russell [5], then later described theoretically by Korteweg and de Vries (KdV) [6]. The KdV approximation assumes a small amplitude perturbation with a long wavelength in a continuous medium. The shape of the solitons in the KdV model is retained due to counterbalance of dispersion (which spreads the wave) and nonlinearity (which steepens or focuses it). Solitons have been found to exist in an ion-electron plasma [7,8]. Compressional, or "bright" solitons have previously been observed in complex plasmas [9], however rarefactional perturbations have not evolved into dark solitons [10]. Both bright and dark solitons (compressional and rarefactive solitons, respectively) have been known to exist in other media such as Bose-Einstein condensates [11], optical waveguides [12,13], and fluids [14]. A large number of theoretical models have been suggested for solitons in complex plasmas [15,16], among many others (see [17] for further references).

Collisions of solitary waves have been extensively studied in liquids theoretically [18,19] and experimentally [14]. It has been reported that solitons on shallow water interact elastically (in KdV approximation) or nearly elastically for the full set of Euler equations. A counterpropagating collision [14] results in a phase lag (delay) of both solitons with the smaller soliton delayed more significantly than the larger one. The amplitude of the overlapping waves is greater than the algebraic sum of the individual solitons before the collision. In addition to that, the amplitude slightly dips immediately after the collision and returns to its value before the collision at a later time. The magnitude of the phase shift reportedly depends on the initial wave amplitudes [20] with larger amplitudes causing larger delays.

Interaction of solitons is interesting in relation to the Fermi-Pasta-Ulam problem (outlined in Ref. [13]). The observation that a discrete nonlinear system exhibits recurrent states instead of an ergodic behavior was explained by Zabusky and Kruskal [7,8] who realized that the nonlinear chain is described by the KdV equation in the continuum

limit (the fact that we also rely upon in our treatment of complex plasmas [9,15,21]). Thus any deviation from the KdV approximation in real systems will affect the thermalization time and break the recurrence of the initial state.

Here we report an experimental and numerical study of interaction of two equal amplitude counterpropagating compressional (bright) solitons in a monolayer complex plasma. The experiment (Fig. 1) was performed in a vacuum chamber which was kept at a pressure of 1.4 Pa by a steady argon flow of 3 sccm. A capacitively coupled 13.56 MHz radio-frequency power of 1 W was applied between the lower powered electrode (20 cm in diameter) and the grounded chamber. Due to the asymmetry of the electrodes the powered electrode had a dc self-bias voltage of −33 V. Plastic microspheres with a diameter of 9.19 ± 0.1 μm were introduced into the plasma, where they charged up and levitated in the sheath above the electrode forming a monolayer hexagonal lattice. The presence of neutral argon gas in the chamber causes the plastic microspheres to experience a small amount of damping. A rim around the outer edge of the lower electrode confined the particles radially. The particle cloud was 64 mm in diameter.

A thin sheet of light from a diode-pumped solid-state laser (532 nm, 300 mW) illuminated the particle layer horizontally from a window on the side of the chamber, while a high-speed digital camera recorded the kinetic motion of the particles from above at a rate of 500 frames/s. The camera's field of view captured a 28.7×28.7 mm^2 (1024 pixel
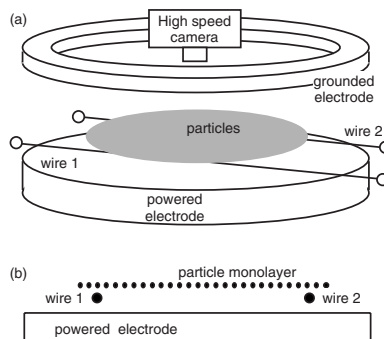
FIG. 1. Sketch of the apparatus. (a) Oblique view showing the microspheres levitating above the lower electrode and forming a monolayer lattice. (b) Side view showing the two wires placed beneath the monolayer. Waves are excited by applying short negative pulses to the wires.

TABLE I. Parameters of the compressional waves obtained in the experiment for different excitation voltages at 0.2 s before the collision (five-frame average). The wave amplitude is calculated as the maximum compression factor, the pulse width is taken at half the maximum amplitude.

Excitation voltage (V)	Amplitude $A = n/n_0$	Width L (mm)	Wave speed V (mm/s)	Mach number M	Soliton parameter AL^2
20	0.63 ± 0.08	4.03 ± 0.50	32.8 ± 1.8	2.5	10
25	0.72 ± 0.04	4.33 ± 0.91	35.8 ± 2.6	2.7	14
30	0.46 ± 0.08	3.98 ± 1.02	38.3 ± 2.1	2.9	8
35	0.32 ± 0.08	3.52 ± 0.58	40.0 ± 2.0	3.0	4
40	0.70 ± 0.23	2.30 ± 0.51	42.5 ± 2.8	3.2	4

$\times 1024$ pixel) region of the crystal lattice. The centers of the field of view, of the electrode, and of the lattice were aligned.

Two parallel tungsten wires, both 0.1 mm in diameter were situated horizontally below the particle layer, at a distance of 25.5 mm on both sides from the center of the electrode (51 mm apart). Both wires were normally grounded to minimize their influence on the particles. Two equal amplitude compressional waves were excited in the particle lattice by applying a brief negative potential lasting 100 ms to both wires simultaneously. A time interval of 100 s allowed the lattice to come to an equilibrium between experimental runs. The pulse amplitude ranged between -20 and -40 V. The average number density of the lattice n_0 at equilibrium was measured for each experiment and found to be 1.57 ± 0.1 mm^{-2}. It was uniform in all directions. The average interparticle spacing was 0.84 mm for all experiments. The dust-lattice wave speed was 13.3 ± 1.6 mm/s. Parameters of observed pulses are listed in Table I.

A molecular dynamics (MD) simulation was performed in order to understand and interpret the experimental results. The three-dimensional equations of motion [9] were solved using the fifth-order Runge-Kutta integration with the Cash Karp adaptive step size control. We used a monolayer lattice formed of 3000 particles in a three-dimensional parabolic confinement potential $\Phi_c = m\Omega_v^2 z^2/2 + m\Omega_h^2(x^2 + y^2)/2$. The lattice was strongly confined in the vertical direction ($\Omega_v = 50$ Hz) and weakly in the horizontal plane ($\Omega_h = 0.5$ Hz). Since the charge and the screening length were not measured in the experiment we chose typical values reported in Refs. [9,10]. The particles with the charge $Q = 16\,000e$ (where e is the electron charge) and mass of $m = 5 \times 10^{-13}$ kg interacted with each other via a screened Coulomb (Yukawa) potential with a screening length $\lambda_D = 1$ mm and their motion was damped by neutral gas friction with a damping constant of 1 Hz. The particle charge and screening length were kept constant during the simulations. The grains were initially placed at random positions and allowed to equilibrate by running the code until a stable hexagonal lattice 9 cm in diameter was formed. The unperturbed number density was inhomogeneous: $n_0 = 0.7$ mm^{-2} at the center of the crystal and it decreased to 0.64 mm^{-2} at the edge of the analyzed region (34×34 mm^2). The particle separation was between 1.28 and 1.35 mm, which corresponded to the screening parameter κ (interparticle distance divided by the Debye length) of 1.28–1.35. The dust-lattice wave speed was between 17.5 and 18.5 mm/s in the analyzed central part of the lattice, which is close to that measured in the experiment. The boundaries of the lattice were assumed to be free. The crystal was then excited by two pulsed Gaussian force fields directed inwards with the maxima separated by 34 mm. The amplitude was chosen so that it produced the same particle speeds as in the experiment. The temporal shape of the excitation pulse was an inverted truncated parabola with a duration of 130 ms (defined as full width at half maximum of the pulse). This produced a pair of counterpropagating waves similar to those observed in the experiment. Parameters of the observed waves are listed in Table II.

In order to analyze the experimental data recorded as a series of still frames, the positions of each particle in all video frames were identified using an intensity weighted moment method [22,23]. All particle positions were then traced from one frame to the next to obtain the velocities of each particle. The local two-dimensional lattice number density was determined as the inverse area of the Voronoi cells for both experiment and simulation. The compression factor was determined as the ratio of the wave number density to the unperturbed number density.

TABLE II. Parameters of the simulated compressional waves 0.2 s before the collision for different excitation forces. The wave amplitude is calculated as the maximum compression factor, the pulse width is taken at half the maximum amplitude.

Excitation force F (arb. units)	Amplitude $A = n/n_0$	Width L (mm)	Wave speed V (mm/s)	Mach number M	Soliton parameter AL^2
3	1.8 ± 0.1	2.5 ± 0.2	30 ± 1	1.67	11
5	2.3 ± 0.1	2.2 ± 0.2	32 ± 2	1.78	11
7.5	3.6 ± 0.1	2.1 ± 0.2	38 ± 1	2.1	16
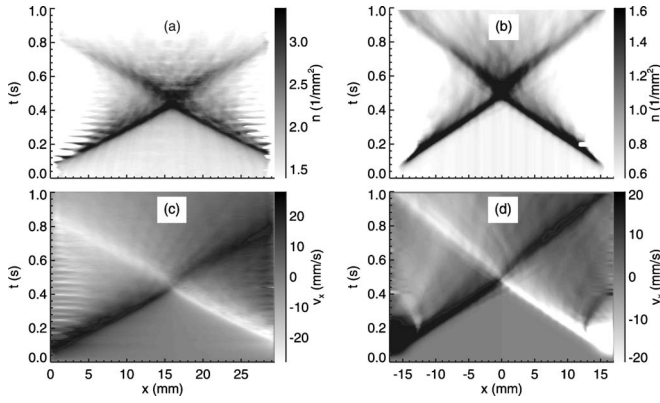
FIG. 2. Trajectories of interacting waves produced from the number density n in the (a) experiment and (b) simulation, as well as from the x component of particle velocity v_x in the (c) experiment and (d) simulation. The excitation amplitude was −40 V in the experiment and 8 arb. units in the simulation. The wave fronts are represented by crossing stripes. The interaction results in a temporal delay after the collision (see Fig. 3 for more details).

The experimental and simulational data were visualized by plotting the grayscale maps of the particle number density and the x velocity (in the direction perpendicular to the wires) as functions of x coordinate and time. In these coordinates wave phenomena look as straight lines with the slope depending on the propagation speed. The counterpropagating wave trajectories are then represented by two crossing stripes (Fig. 2). It should be noted that the wave amplitude slightly decreases in time due to neutral damping as reported in Ref. [9]. It appears that there is a small temporal delay between converging (lower part of the plots) and diverging (upper part of the plots) waves. The angles of the stripes indicate that the diverging waves propagate slightly slower than the converging ones. This is more likely to be an effect of the neutral damping (which reduces the wave amplitude and slows them down) than the wave interaction.

In order to measure the propagation delay of the waves we fitted their trajectories with straight lines separately before and after the collision obtaining two pairs of lines (Fig. 3). The lines cross at two different points. The delay time Δt was determined from the offset between the crossing points. It was then plotted vs excitation amplitude for experimental
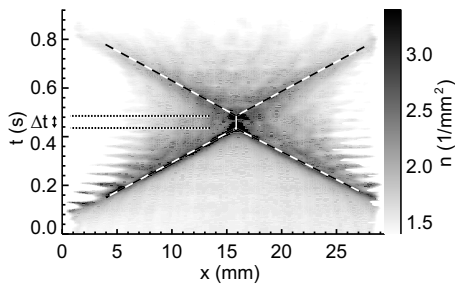
FIG. 3. Temporal offset observed in the paths of two compressional waves from the visualization of the double wire experiment with pulse amplitude −40 V. Plot shows time versus distance, where darker regions correspond to an increase in number density. Temporal delay is obtained at the point of collision.
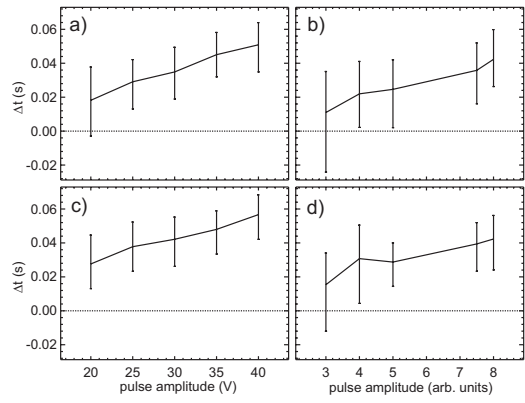
FIG. 4. Soliton interaction temporal delay as a function of the excitation amplitude. The delays obtained from the number density in the (a) experiment and (b) simulation coincide with those obtained from the particle x velocity in the (c) experiment and (d) simulation.

and simulational data in Fig. 4. We used both number density and particle x-velocity data to obtain the delay time which was positive in all our experimental and simulational runs. The error bars were estimated from the widths and lengths of the wave trajectories which limit the precision of the fits. We have found that the delay time increased with the excitation amplitude.

The soliton parameter AL^2 was measured for each frame of the video recording, where A and L are, respectively, the wave amplitude (maximum compression factor) and its width taken at half the maximum amplitude. Following the KdV theory, this value should be almost constant in weakly damped inhomogeneous case [9]. It was observed in each experiment that AL^2 became increasingly steady before the collision, reaching an equilibrium value. However, with increasing pulse amplitude the soliton parameter appeared to be taking longer to reach a steady value. It was also observed that the soliton parameter is reduced (Table I) at large amplitudes (35–40 V excitation), this is most likely due to breaking of the KdV approximation, which assumes that the amplitude of nonlinear waves is small, that the wavelength is large, and that the lattice is continuous. All these three assumptions will break as the excitation amplitude is increased.

In order to underline the nonlinear interaction of the counterpropagating waves, we ran other simulations in the same crystal with only one pulse propagating in either positive or negative x direction. We noticed that the amplitude of the single pulse was decreasing as it propagated through the lattice because of damping. Moreover the amplitude of two colliding waves was less than the sum of the amplitudes of individual noninteracting pulses taken at the same time. After the collision, the propagation velocities in the double pulse simulation were also slightly smaller than those in the single pulse cases, most likely because double pulses propagate in the lattice perturbed by the other pulse.

The observed nonlinear waves propagate faster (see Tables I and II) than linear compressional dust-lattice waves, the soliton parameter is conserved (at small amplitudes after it has reached an equilibrium value), the waves are delayed after a collision, and they re-emerge in their original shape
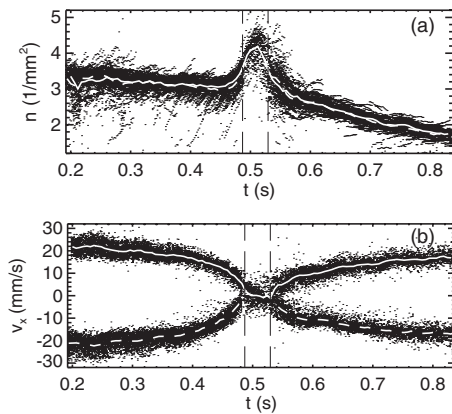
FIG. 5. Interaction of two counterpropagating solitons of equal amplitude in the experiment with −30 V excitation pulse. Soliton amplitude in (a) local number density and (b) particle x velocity. The black dots are the data along the narrow stripes at the soliton maxima (Fig. 3). The solid and dashed lines are boxcar averages over three data points in time. The solid (dashed) line represents the soliton traveling in the positive (negative) direction. The vertical lines represent the begin and end times of the collision, when the solitons appear merged together.

after a collision. For these reasons, we can consider the waves as solitons (see also [9]).

The propagation delay observed in our experiments and MD simulations increases with the initial amplitude of the colliding solitons. These results are in qualitative agreement with the prediction done for the KdV model [20]. However the precision of our measurements is not high enough to check whether the delay is proportional to the square root of the initial amplitude.

The interaction of the solitons in the experiment with −30 V excitation pulse is presented in Fig. 5, which shows the time evolution of (a) the soliton maximum number densities and (b) the maximum particle x velocities. This figure was obtained by fitting the soliton maxima with straight lines (Fig. 3) and then selecting the data points that were within ± 0.25 mm of each line (the soliton width was larger than 3

mm). The selected values of number density and x velocity were plotted as black points. In order to reduce the scatter we averaged the data in three adjacent video frames (dashed and solid lines). The number density amplitude of the solitons increases during the interaction by a factor of 1.4 [Fig. 5(a)], while the particle x velocity remains nearly zero for the time of interaction [Fig. 5(b)]. Note that the amplitude of the solitons away from the collision point decreases with time due to neutral damping [9].

Our experiment shows that the amplitude of the overlapping solitons is 1.4 times the initial amplitude of the colliding solitons for the excitation pulse of −30 V. This is less than a linear superposition of the amplitudes of colliding solitons. It is also less than the predictions based on the second- and third-order perturbation theory (which are even higher than the linear superposition) [24]. In contrast to our observations the fluid dynamic experiments and simulations reported superlinear amplitudes of the interacting solitons (run up) [18] consistent with the theory of Ref. [24]. We have no explanation for this, however it is likely that the KdV model becomes inadequate due to excessive amplitude of the lattice perturbation, or that the discrete nature of the lattice has to be taken into account. We do not observe any dip in the soliton amplitude after the collision nor any oscillatory residual. However the resolution of the experimental data is limited by the statistical noise due to random motion of the lattice. The noise level incurred is most likely too high to observe such residuals.

This study has shown the effect of a head-on collision of two parallel wave fronts in a complex plasma. In each experiment performed, the interaction of the soliton waves had produced a temporal delay in propagation, which increased with the initial amplitude of the solitons, in qualitative agreement with theoretical predictions and fluid dynamics experiments. The observed amplitude of the overlapping solitons was smaller than the theoretically predicted value. The effects of this experiment have been reproduced in a molecular dynamics simulation.

[1] H. Ikezi, Phys. Fluids **29**, 1764 (1986).
[2] H. Thomas *et al.*, Phys. Rev. Lett. **73**, 652 (1994).
[3] Y. Hayashi and K. Tachibana, Jpn. J. Appl. Phys., Part 2 **33**, L804 (1994).
[4] J. H. Chu and L. I, Phys. Rev. Lett. **72**, 4009 (1994).
[5] J. Robinson and J. Russel, in *Report of the Committee on Waves*, Report Seventh Meeting of British Association for the Advancement of Science (John Murray, London; Liverpool, 1838), p. 417.
[6] D. Korteweg and G. de Vries, Philos. Mag. **39**, 422 (1895).
[7] N. J. Zabusky and M. D. Kruskal, Phys. Rev. Lett. **15**, 240 (1965).
[8] M. Q. Tran, Phys. Scr. **20**, 317 (1979).
[9] D. Samsonov *et al.*, Phys. Rev. Lett. **88**, 095004 (2002).
[10] T. E. Sheridan *et al.*, Phys. Plasmas **15**, 073703 (2008).
[11] B. Jackson *et al.*, Phys. Rev. A **75**, 051601(R) (2007).

[12] M. Segev, Opt. Quantum Electron. **30**, 503 (1998).
[13] F. Lederer *et al.*, Phys. Rep. **463**, 1 (2008).
[14] T. Maxworthy, J. Fluid Mech. **76**, 177 (1976).
[15] I. Kourakis and P. K. Shukla, Eur. Phys. J. D **29**, 247 (2004).
[16] N. Rao and P. Shukla, Planet. Space Sci. **42**, 221 (1994).
[17] G. E. Morfill and A. V. Ivlev, Rev. Mod. Phys. **81**, 1353 (2009).
[18] W. Craig *et al.*, Phys. Fluids **18**, 057106 (2006).
[19] T. Marchant and N. Smyth, IMA J. Appl. Math. **56**, 157 (1996).
[20] M. Oikawa and N. Yajima, J. Phys. Soc. Jpn. **34**, 1093 (1973).
[21] S. K. Zhdanov *et al.*, Phys. Rev. E **66**, 026411 (2002).
[22] Y. Feng *et al.*, Rev. Sci. Instrum. **78**, 053704 (2007).
[23] Y. Ivanov and A. Melzer, Rev. Sci. Instrum. **78**, 033506 (2007).
[24] C. Su and R. Mirie, J. Fluid Mech. **98**, 509 (1980).